

1997

The Effects of Organic Compounds on Inhibition of Hydrogen Permeation Through a Mild Steel Membrane

H. A. Duarte

University of South Carolina - Columbia

D. M. See

University of South Carolina - Columbia

Branko N. Popov

University of South Carolina - Columbia, popov@enr.sc.edu

Ralph E. White

University of South Carolina - Columbia, white@cec.sc.edu

Follow this and additional works at: https://scholarcommons.sc.edu/eche_facpub

 Part of the [Chemical Engineering Commons](#)

Publication Info

Journal of the Electrochemical Society, 1997, pages 2313-2317.

This Article is brought to you by the Chemical Engineering, Department of at Scholar Commons. It has been accepted for inclusion in Faculty Publications by an authorized administrator of Scholar Commons. For more information, please contact digres@mailbox.sc.edu.

The Effects of Organic Compounds on Inhibition of Hydrogen Permeation Through a Mild Steel Membrane

H. A. Duarte,* D. M. See, B. N. Popov,** and R. E. White**

Department of Chemical Engineering, University of South Carolina, Columbia, South Carolina 29208, USA

ABSTRACT

The effectiveness of 5-(4-pyridyl)-2,7-nonadiene, and 1 phenyl-2-propyn-ol (PP) on inhibition of the hydrogen evolution reaction on a 1010 steel membrane and on the degree of hydrogen ingress into the membrane was determined. Hydrogen evolution rates and permeation currents were monitored as a function of time at different applied potentials. In the presence of 0.5 g/liter PP in the electrolyte, the hydrogen discharge and permeation current density were inhibited by 98 and 95%, respectively.

Introduction

Hydrogen can cause embrittlement of metals and alloys during electroplating, cathodic protection, and corrosion of metals.¹⁻⁴ Various methods have been proposed to decrease hydrogen embrittlement.⁵⁻⁹ However, it is usually impossible to reduce hydrogenation of metals and alloys to a level that eliminates the possibility of hydrogen cracking. According to our earlier studies,¹⁰⁻¹⁹ an alloy surface modification with underpotentially deposited metals (Zn, Bi, Pb) or deposited Zn or Bi inhibits the hydrogen discharge reaction and reduces drastically the degree of hydrogen ingress in the substrate.

Corrosion inhibitors were also used to decrease the hydrogen permeation and embrittlement effects.¹⁹⁻²² Martin²³ found that all three states of H in steels, mobile, reversibly trapped, and irreversibly trapped were minimized in quantity when inhibitors were used to mitigate corrosion. According to Wilhelm *et al.*²⁴ diamines with long carbon chains were most effective in reducing the corrosion rate and hydrogen adsorption.

The objective of this study was to investigate the effect of two organic compounds 1-phenyl-2-propyn-1-ol (PP) and 5-(4-pyridyl)-2,7-nonadiene (PN) on the hydrogen permeation through a mild steel membrane.

Experimental

The Devanathan-Stachurski permeation technique^{25,26} was used to investigate the rate of hydrogen permeation through a 1010 steel with an area of approximately 0.4 cm² with thickness of 0.03 cm. The experiments were carried out in a system with two compartments, separated by a bipolar membrane made of 1010 steel. Prior to the experiment, the membrane was prepared by polishing with 0.5 μm high purity alumina powder and cleaning in an ultrasonic cleaning bath. Just prior to placing the membrane in the permeation cell, it was etched for 20 s in a methanol solution containing 1% H₂SO₄, rinsed with deionized water, and then dried in the air.

The electrolyte on the cathodic side of the cell was 0.5 M HCl. The rate of hydrogen permeation through the alloy in the absence and presence of 0.5 g/liter of PN or PP was recorded continuously as a function of time. The electrolyte on the anodic side of the cell was 0.2 M NaOH. To keep electrolyte impurities at the lowest possible level, the solutions for the anodic and cathodic compartments were pre-electrolyzed at least 24 h in a separate electrolytic cell prior to introduction into the compartment. The potential of the "diffusion side" of the membrane (the side from which the hydrogen emerged) was set at a value that corresponded to a practically zero concentration of the absorbed atomic hydrogen on the surface.²⁶ This condition was maintained by the instantaneous ionization of all hydrogen atoms that diffused through the membrane and emerged on the diffusion side.

To avoid passivation or dissolution of the metal, the anodic side of the steel membrane was always electroplated with a thin layer (0.15 to 0.2 μm) of palladium. It was assumed in this work that this thin film of palladium would not affect the permeation rate of hydrogen through the steel membrane because it is well known that hydrogen diffuses rapidly through palladium. The deposition was carried out in an electrolyte containing 2 × 10⁻⁶ M sodium tetranitropalladium [Na₂Pd(NO₂)₄] using a current density of 200 μA/cm² for 4 h. Then, the electrolyte was drained off, and the compartment was washed with deionized water and filled with 0.2 M NaOH. The solution was kept at -0.3 V vs. Hg/HgO reference electrode until the background current was reduced below 0.03 μA/cm². Then the cathodic compartment was filled with a supporting electrolyte containing 0.5 M HCl. The membrane was then saturated with hydrogen to fill possible irreversible trapping sites in the membrane by keeping the cathodic side applied potential of -0.8 V vs. SCE until the measured permeation current was constant. Prepurified nitrogen was bubbled through both compartments to keep them free of dissolved oxygen. All experiments were carried out at constant volume, inhibitor concentration, temperature, pressure, and substrate surface area.

Results and Discussion

Permeation experiments were performed to clarify the role of organic inhibitors (PP and PN) on hydrogen entry kinetics in acidic media. To determine the hydrogen entry kinetics into C-1010 steel, experiments were carried out in 0.5 M HCl to measure the cathodic current density and the permeation current density as a function of the applied overpotential. In these experiments, the alloy membrane on the cathodic site of the cell was polarized potentiostatically. The hydrogen permeation transient into a bipolar membrane in a diffusion mode can be presented by the following equations obtained for two typical boundary conditions: (i) for the case where the hydrogen concentration at the entry side of the membrane is constant²⁷

$$\frac{j_t - j_o}{j_x - j_o} = 1 + 2 \sum_{n=1}^{\infty} (-1)^n e^{-n^2 \pi^2 \tau} \quad [1]$$

(ii) for the case where the flux of the hydrogen entering the membrane is constant²⁸

$$\frac{j_t - j_o}{j_x - j_o} = 1 - \frac{4}{\pi} \sum_{n=1}^{\infty} \frac{(-1)^n}{(2n+1)} e^{-\frac{(2n+1)^2 \pi^2 \tau}{4}} \quad [2]$$

where j_t is the transient hydrogen permeation current density, j_x is the steady-state hydrogen permeation current density, j_o is the initial hydrogen current density, and $\tau = tD/L^2$, where t is time, L is the membrane thickness, and D is the hydrogen diffusivity.

Equations 1 and 2 are compared in Fig. 1 to our experimental permeation curve for a 1010 steel membrane (obtained in the absence of inhibitor in the electrolyte). As shown in Fig. 1 the experimental permeation curve is clos-

* Electrochemical Society Student Member.

** Electrochemical Society Active Member.

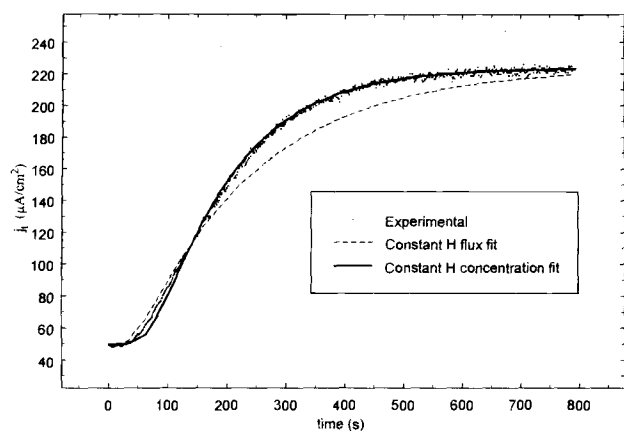


Fig. 1. The comparison of the experimental transient of hydrogen permeation current density with two typical theoretical solutions.

er to the theoretical curve given by Eq. 1. The diffusion coefficient was evaluated by two different methods. In the first method, Eq. 1 was fitted using a computer program to the experimental data to find $D = 7.2 \times 10^{-7} \text{ cm}^2/\text{s}$, using $j_s = 223 \mu\text{A}/\text{cm}^2$, and $j_o = 50 \mu\text{A}/\text{cm}^2$ from Fig. 1, and $L = 0.03 \text{ cm}$. The second method, which consisted in using $t_{1/2} = 0.138L^2/D$,²⁹ where $t_{1/2}$ (172 s) is the time corresponding to half rise of the permeation curve, yielded the same value for the hydrogen diffusivity. The diffusion coefficient valued obtained in this work is consistent with the previously obtained value for the hydrogen diffusion coefficient in AISI 4340 steel.¹²

The effect of the inhibitors on the cathodic current density at different applied potentials is shown in Fig. 2, which shows that the cathodic current density is much lower in the presence of 0.5 g/liter of PP or 0.5 g/liter of PN in the electrolyte. Our previous studies using a rotating disk electrode have shown that the optimum concentration for corrosion inhibition of C-1010 steel for both inhibitors is 0.5 g/liter.³⁰ At -0.9 V vs. SCE , the hydrogen cathodic current density in the presence of 0.5 g/liter of PP is $2 \text{ mA}/\text{cm}^2$ compared with $90 \text{ mA}/\text{cm}^2$ measured on a bare alloy membrane. The inhibition efficiencies of 0.5 g/liter of PP and PN at different applied potentials are presented in Fig. 3. The inhibitor inhibition efficiency is defined as $P_i = (i_c - i_i)/i_c$, where i_c is the cathodic current density measured in the absence of the inhibitor and i_i is the cathodic current density measured in the presence of inhibitor. As shown in Fig. 3, the hydrogen discharge current at -0.6 V vs. SCE was reduced by 80 and 98% in the presence of PN and PP, respectively. The results indicated that both inhibitors adsorb on the surface of the electrode and

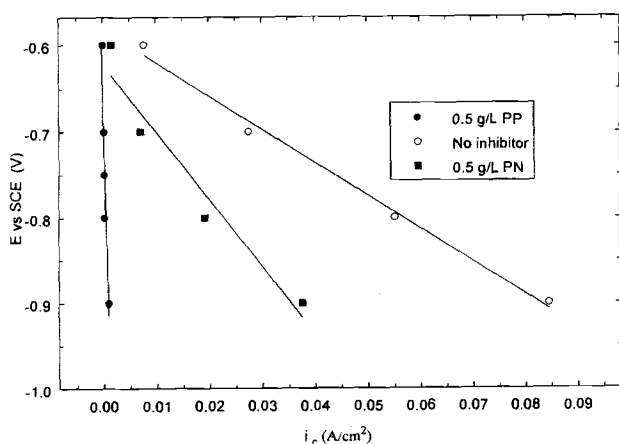


Fig. 2. The effect of PN and PP on the cathodic current density as a function of the applied cathode cell potential. $C_{\text{PN}} = 0.5 \text{ g/liter}$, $C_{\text{PP}} = 0.5 \text{ g/liter}$ in 0.5 M HCl .

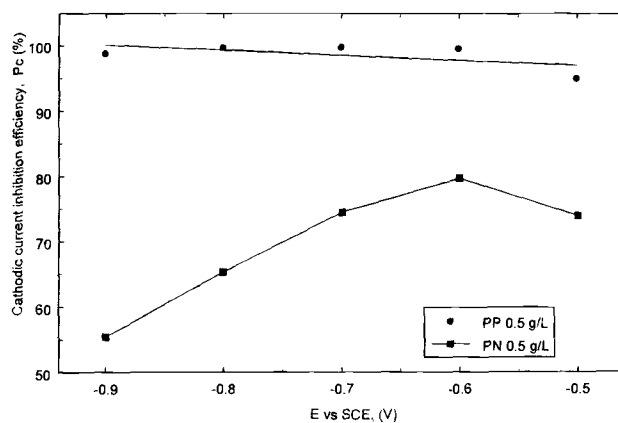


Fig. 3. The cathodic current inhibition efficiency of PN and PP vs. applied potential E .

inhibit the hydrogen discharge reaction. Adsorbed PN and PP molecules decrease the cathodic reaction sites of the electrode.

The hydrogen permeation current was measured in the presence and absence of inhibitors. At the beginning of the permeation experiment, the cathodic side of the membrane was held at a potential of -0.6 V vs. SCE . The potential was then stepped to more negative values of -0.7 , -0.8 , and -0.9 V vs. SCE and the steady-state permeation curve was recorded as a function of time. The resulting permeation transients obtained at -0.6 , -0.7 , -0.8 , and -0.9 V vs. SCE are shown in Fig. 4. With inhibitors present on the surface of the electrode, the hydrogen permeation current decreases drastically at all tested potentials. The effect of 0.5 g/liter PN and 0.5 g/liter PP on the hydrogen permeation current is presented in Fig. 5 as a function of the applied potential. The lines represent the linear regression fit to the data. As shown in Fig. 5, the hydrogen permeation current is lower in the presence of inhibitors. At -0.9 V vs. SCE , the hydrogen permeation current in the absence of inhibitors was $150 \mu\text{A}$. In the presence of 0.5 g/liter of PN and 0.5 g/liter PP the hydrogen permeation currents were: 97 and $5 \mu\text{A}$, respectively. The permeation current inhibition efficiencies of PN and PP were defined as $P_j = (j_i - j_i)/j_i$, (where j_i is the transition permeation current in the absence of inhibitor and j_i is the permeation current in the presence of inhibitor), and are presented in Fig. 6 as a function of the applied potential at the cathodic side of the membrane. At -0.9 V vs. SCE in the presence of PN and PP in the electrolyte, the hydrogen permeation current inhibition efficiencies are 35 and 95%, respectively. PN inhibits the permeation current more efficiently at lower applied potentials. As shown in Fig. 6, at -0.6 V vs. SCE the PN

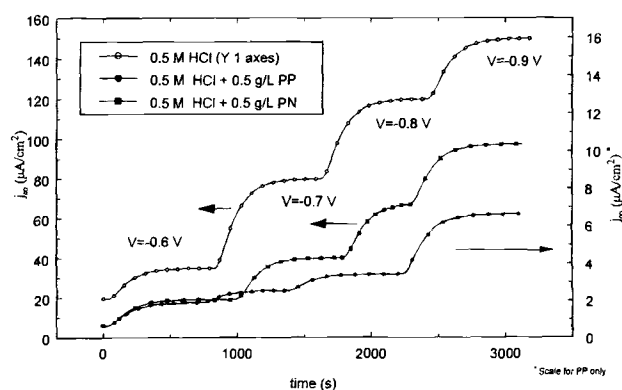


Fig. 4. Hydrogen permeation transients through a 1010 steel membrane at different applied potentials in the absence and presence of inhibitors. The membrane thickness is 0.03 cm .

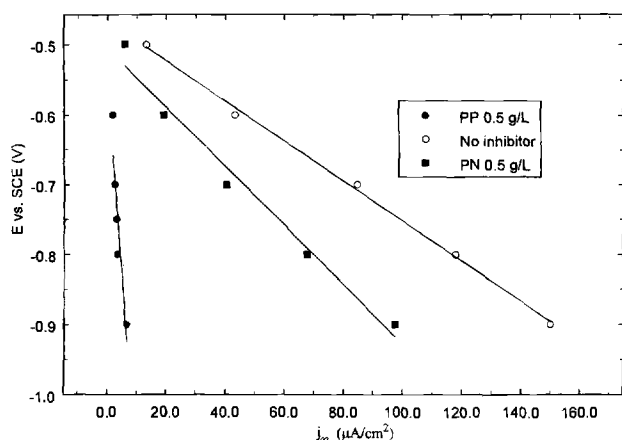


Fig. 5. The effect of the inhibitors on the hydrogen permeation transients as a function of the applied cell potential.

permeation current inhibition efficiency increases up to 55%.

An attempt was made using the IPZ model to quantify the effect of the organic inhibitor on the hydrogen permeation process. The mechanistic model of Iyer *et al.*³¹ was used to determine the surface concentration and the hydrogen surface coverage, the hydrogen absorption, discharge, and recombination rate constants as well as HER coverage-dependent transfer coefficient, α , and the exchange current density i_0 from a knowledge of the steady-state hydrogen permeation current, cathodic current, hydrogen diffusivity, and hydrogen overvoltage.

The IPZ model assumes that (i) the hydrogen reaction occurs via the coupled discharge-recombination mechanism, (ii) the recombination step of hydrogen is not rate-determining so that the hydrogen atom oxidation can be neglected, ($\eta \gg RT/F$), (iii) the Langmuir isotherm is used to describe the hydrogen coverage of the substrate, (iv) the intermediate hydrogen adsorption-absorption reaction is in local equilibrium, and (v) the hydrogen permeation process is described by a simple diffusion model through the membrane. With these assumptions one can derive the following relationships⁹

$$i_c = i_0'(1 - \theta_H)e^{-\alpha a \eta} \quad [3]$$

$$i_r = Fk_3\theta_H^2 \quad [4]$$

$$j_x = \frac{k''\theta_H}{b} \quad [5]$$

$$j_x = \frac{k''}{b\sqrt{Fk_3}}\sqrt{i_r} \quad [6]$$

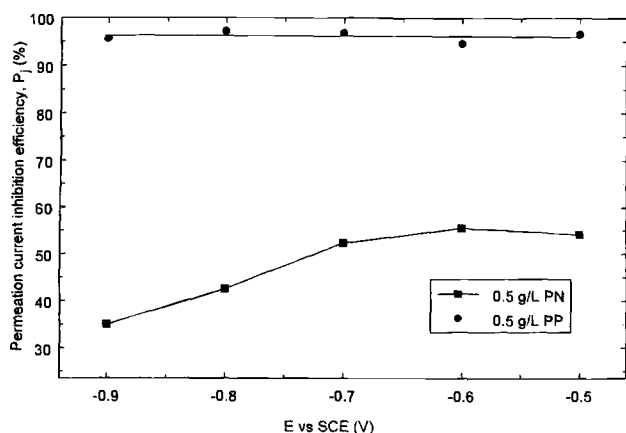


Fig. 6. The permeation current inhibition efficiencies of PN and PP vs. E.

$$i_c e^{a\eta} = -\frac{bi_0'}{k''}j_x + i_0' \quad [7]$$

where $i_r = i_c - j_x$ is the hydrogen recombination current density, i_c is the cathodic current density, $b = L/FD$, L is the membrane thickness, F is the Faraday constant, D is the hydrogen diffusion coefficient, $a = F/RT$, α is the transfer coefficient, η is the overpotential, R is the gas constant, T is temperature, and θ_H is the hydrogen surface coverage, k_3 is the recombination rate constant, $i_0' = i_0/(1 - \theta_e)$, where i_0 is the exchange current density, θ_e is the equilibrium hydrogen coverage, and k'' is the thickness-dependent adsorption-absorption constant, defined as $k_{\text{abs}}/(k_{\text{ads}} + D/L)$ where k_{abs} is the absorption rate constant for hydrogen into the metal and k_{ads} is the desorption constant for hydrogen from the metal.⁹

The dependence of the steady-state hydrogen permeation current upon the overpotential provided in this study is a diagnostic criterion for the identification of the mechanism of the discharge of hydrogen ions on the steel membrane. The experiments were carried out at a potential region where $\eta \gg RT/F$. In this region it was found that the slope of $-\partial\eta/\partial \log(j_x) = 290$ mV [theoretical value = 273 mV/decade = $2.3 \times 4RT/F$ ($T = 298.15$ K)] which indicates a coupled discharge-recombination mechanism,³² which is one of the assumptions for the applicability of the model.

Figures 7, 8, and 9 show the dependence of the steady-state permeation current upon the square root of the recombination current density in the absence of inhibitor and in the presence of 0.5 g/liter PN and 0.5 g/liter PP, respectively. The linear regression curves are shown as continuous lines in the figures and indicate that the per-

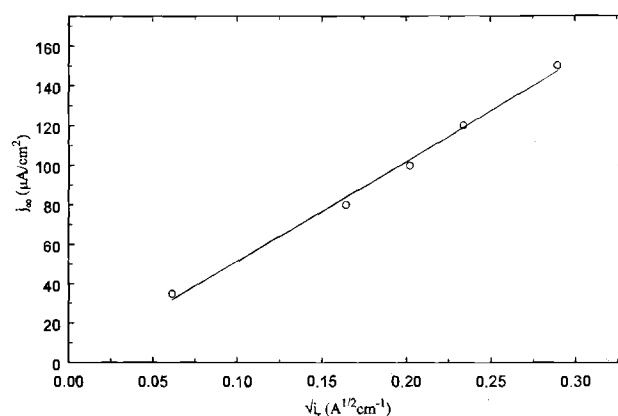


Fig. 7. The steady-state hydrogen permeation current density, j_{∞} , for the bare iron vs. the square root of the recombination current density, $\sqrt{i_r}$.

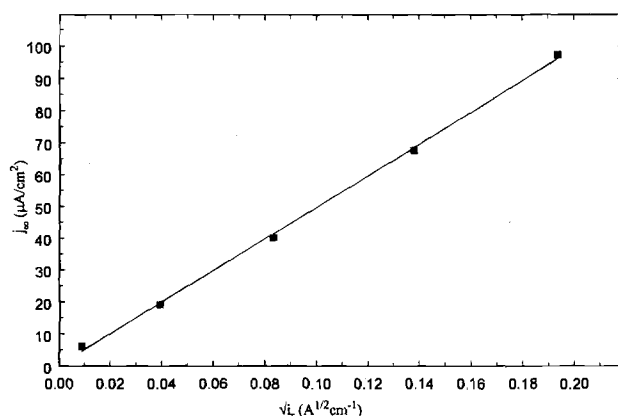


Fig. 8. The steady-state hydrogen permeation current density, j_{∞} , obtained in the presence of 0.5 g/liter PN vs. the square root of the recombination current density, $\sqrt{i_r}$.

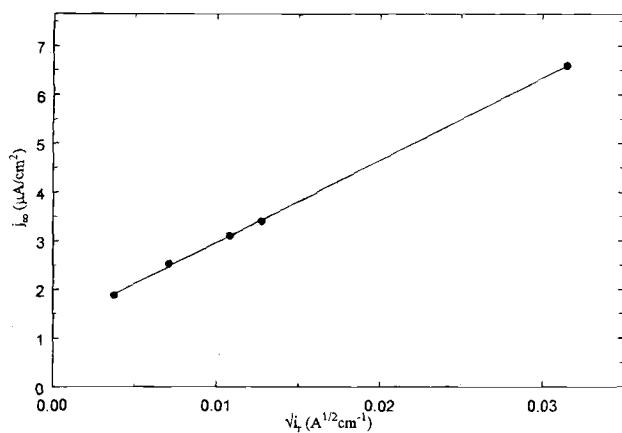


Fig. 9. The steady-state hydrogen permeation current density, j_{per} , obtained in the presence of 0.5 g/liter PP vs. the square root of the recombination current density, $\sqrt{i_r}$.

meation rate is significantly lower when inhibitors were present in the electrolyte. The observed linear relationship of hydrogen permeation current upon the square root of the recombination current in the absence and presence of inhibitors is consistent with Eq. 6.

The permeation current densities, j_{per} , vs. the charging function, $i_c e^{\alpha n}$, in the absence and presence of PN are presented in Fig. 10. Figure 11 shows the same relationship but in the presence of PP in the electrolyte. Using the slopes and intercepts in Fig. 7 through 11 and Eq. 6 and 7,

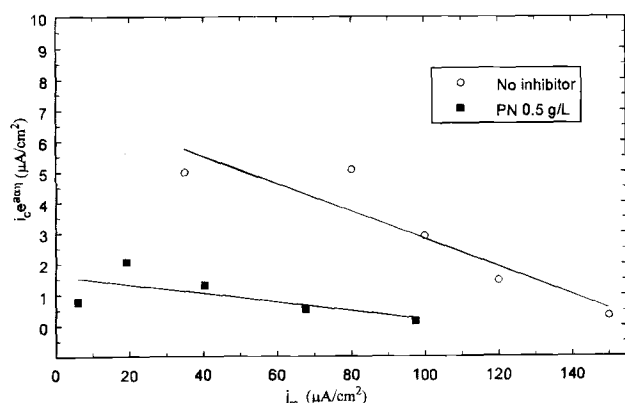


Fig. 10. The steady-state hydrogen permeation current density, j_{per} , vs. charging function, $i_c e^{\alpha n}/RT$ obtained in the absence of inhibitor and in the presence of 0.5 g/liter PN.

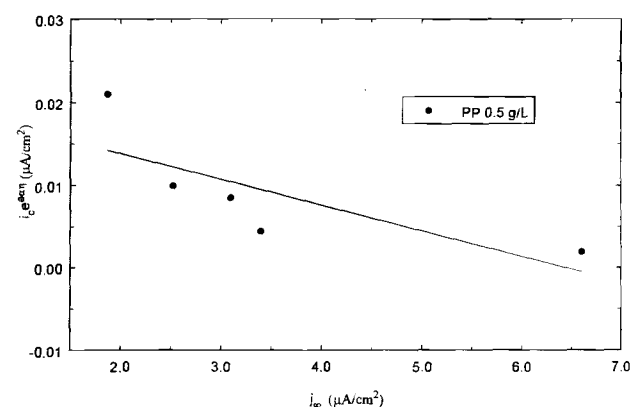


Fig. 11. The steady-state hydrogen permeation current density, j_{per} , vs. charging function, $i_c e^{\alpha n}/RT$ obtained in the presence of 0.5 g/liter PP.

Table I. IPZ model results.

Electrolyte/Parameter	i_0' (A cm ⁻²)	k'' (mol cm ⁻³)	k_3 (mol cm ⁻² s ⁻¹)
0.5 M HCl	7.3×10^{-6}	7.02×10^{-5}	1.07×10^{-6}
0.5 M HCl + 0.5 g/liter PP	4.7×10^{-8}	1.93×10^{-6}	7.43×10^{-9}
0.5 M HCl + 0.5 g/liter PN	1.6×10^{-6}	3.51×10^{-5}	2.79×10^{-7}

the values of i_0' , k'' , and k_3 were calculated and are presented in Table I. Substituting the recombination constant, k_3 , and the experimentally measured recombination current into Eq. 3, the hydrogen surface coverage was calculated and is presented in Fig. 12. The points were calculated from the IPZ model results at the experimentally tested overpotentials. As shown in Fig. 12, the hydrogen surface coverage decreases drastically in the presence of 0.5 g/liter of PP. The inhibitors cause a suppression of hydrogen surface coverage by adsorbing on the surface thus decreasing the substrate electroactive area for hydrogen discharge reaction. As a consequence, the hydrogen adsorption process is altered without changing the mechanical or physical properties of the substrate.

According to Eq. 5, the hydrogen permeation flux may be reduced by decreasing the hydrogen surface coverage by decreasing the adsorption-adsorption constant. As shown in Table I, both the exchange current density and the adsorption-adsorption constant decrease in the presence of inhibitors. The decrease in the exchange current density accounts for the decrease in the cathodic current and consequently in a decrease of the hydrogen permeation current. PN reduces the hydrogen permeation rate by reducing the amount of hydrogen that discharges at the electrode surface, while PP reduces both the exchange current density and the adsorption-adsorption constant. Thus, the presence of PP in the electrolyte decreases the hydrogen discharge current and hydrogen permeation even at high cathodic potentials, up to 98 and 95%, respectively. The observed decrease of the hydrogen discharge and permeation currents in the presence of PP at high cathodic potentials indicates the potential for the use of PP in cathodic protection systems.

Our interpretation of the experimental data is that the model assumptions were reasonable in the potential region in which the inhibitors were studied. Despite the model limitations, we believe it is possible to compare the kinetic parameters in the presence and the absence of the inhibitors to quantify their effect.

It is important to point out that the values of the calculated model dependent parameters are valid as long as the assumptions of the IPZ model are applicable. This interpretation is also restricted to the potential area in which the parameters were estimated.

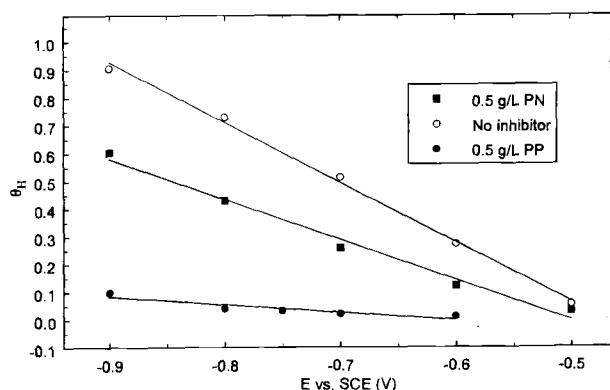


Fig. 12. The hydrogen surface coverage, θ_H , vs. applied potential, E , estimated in the absence of inhibitor and in the presence of 0.5 g/liter PN and 0.5 g/liter PP.

Conclusions

The Devanathan-Stachurski permeation technique was used to determine the hydrogen entry kinetics through an iron membrane in the presence and absence of PN and PP inhibitors. Hydrogen evolution rates and hydrogen permeation rates were followed as a function of time at different applied potentials. The hydrogen discharge current at -0.6 V vs. SCE was reduced by 80 and 98% in the presence of PN and PP, respectively; hydrogen permeation current density was reduced by 55 and 95%, respectively. At -0.9 V vs. SCE in the presence of PN and PP in the electrolyte, the hydrogen permeation current inhibition was 35 and 95%, respectively and the discharge current density were reduced by 55 and 95%. It was found, according to the IPZ model, that PN reduces the hydrogen permeation rate by reducing the amount of hydrogen that discharges at the electrode surface, while PP reduces both, the exchange current density and the hydrogen adsorption-adsorption constant.

Acknowledgment

Technical assistance and financial support by A. John Sedriks, the Office of Naval Research, under Contract No. AAESRT N00014-93-1-1094 are gratefully acknowledged.

Manuscript submitted July 30, 1996; revised manuscript received March 24, 1997.

The University of South Carolina assisted in meeting the publication costs of this article.

LIST OF SYMBOLS

a	F/RT , a constant, V^{-1}
b	$L/(FD)$, a constant, $(A\text{ cm})^{-1}$
C_H	hydrogen surface concentration, mol cm^{-3}
C_H^{max}	maximum hydrogen surface concentration, mol cm^{-3}
D	hydrogen diffusivity, $\text{cm}^2\text{ s}^{-1}$
E_{oc}	open-circuit potential, V
E_c	cathodic potential, V
F	Faraday constant, 96487 C/eq mol
i	current density, A/cm^2
i_c	cathodic current density, A/cm^2
i_r	hydrogen recombination current density, A/cm^2
i_0	exchange current density, A/cm^2
i_i	cathodic current density measured in the presence of inhibitor, A/cm^2
i'_0	$i_0/(1 - \theta_c)$, A/cm^2
j_∞	steady-state hydrogen permeation current density ($j_\infty = FDC_H/L$), A/cm^2
j_0	initial hydrogen permeation current density, A/cm^2
j_i	transition hydrogen permeation current density in the presence of inhibitor, A/cm^2
j_t	transition hydrogen permeation current density, A/cm^2
k_3	recombination rate constant, $\text{mol}(\text{cm}^2\text{ s})^{-1}$
k^n	thickness dependent absorption-adsorption constant, mol cm^{-3}
L	membrane thickness, cm
P_i	inhibitor efficiency $(i_c - i_i)/i_c$, dimensionless
P_j	permeation current inhibitor efficiency $(j_c - j_i)/j_c$, dimensionless
R	gas constant, $8.3143\text{ J}(\text{mol K})^{-1}$
t	time, s
$t_{1/2}$	time corresponding to the half rise of the permeation curve, s
T	temperature, K

Greek

α	transfer coefficient, dimensionless
η	overpotential, V
θ_e	equilibrium hydrogen surface coverage, dimensionless
θ_H	hydrogen surface coverage, dimensionless
τ	t/D^2 , dimensionless time

REFERENCES

1. R. A. Oriani, *Ann. Rev. Mater. Sci.*, **8**, 327 (1978).
2. J. O'M. Bockris and A. K. N. Reddy, *Modern Electrochemistry*, Vol. 2, p. 1231, Plenum Press, New York (1970).
3. J. O'M. Bockris and P. K. Subramanian, *Electrochim. Acta*, **16**, 2169 (1971).
4. R. H. Song and S. Pyun, *This Journal*, **137**, 1051 (1990).
5. B. E. Wilde and T. Shimada, *Scr. Metall.*, **22**, 551 (1988).
6. P. J. Grobner, D. L. Sopnseller, and D. E. Diesburg, *Corrosion*, **35**, 240 (1979).
7. M. Manohar, Ph.D. Thesis, Ohio State University, Columbus, OH (1990).
8. B. E. Wilde and I. Chatteraj, *Scr. Metall.*, **26**, 627 (1992).
9. R. N. Iyer, H. W. Pickering, and M. Zamanzadeh, *This Journal*, **136**, 2463 (1989).
10. B. N. Popov, G. Zheng, and R. E. White, *Corrosion*, **50**, 613 (1994).
11. B. N. Popov, G. Zheng, and R. E. White, *ibid.*, **51**, 429 (1995).
12. B. N. Popov, G. Zheng, and R. E. White, *This Journal*, **140**, 3153 (1993).
13. G. Zheng, B. N. Popov, and R. E. White, *ibid.*, **141**, 1220 (1994).
14. G. Zheng, B. N. Popov, and R. E. White, *ibid.*, **141**, 1526 (1994).
15. B. N. Popov, G. Zheng, and R. E. White, *Corros. Sci.*, **36**, 2139 (1994).
16. G. Zheng, B. N. Popov, and R. E. White, *J. Appl. Electrochem.*, **25**, 212 (1995).
17. G. Zheng, B. N. Popov, and R. E. White, *This Journal*, **142**, 154 (1995).
18. D. H. Coleman, G. Zheng, B. N. Popov, and R. E. White, *ibid.*, **143**, 1871 (1996).
19. R. L. Martin, *Mater. Perform.*, **19**, 20 (1980).
20. K. van Gelder, M. J. Simon Thomas, and C. J. Kroese, *Corrosion*, **42**, 36 (1986).
21. R. L. Martin, *Mater. Perform.*, **13**, 19 (1974).
22. R. L. Martin, *ibid.*, **22**, 33 (1986).
23. R. L. Martin, *Corrosion*, **49**, 694 (1993).
24. S. M. Wilhelm and D. Abayarathna, *ibid.*, **50**, 152 (1994).
25. M. A. V. Devanathan and Z. Stachurski, *Proc. R. Soc. London, Ser. A*, **270**, 90 (1962).
26. M. A. V. Devanathan and Z. Stachurski, *This Journal*, **110**, 886 (1963).
27. M. A. V. Devanathan, *Tech. Rep. ONR/551/22NR-036-028*, Office of Naval Research, Washington, DC (1961).
28. N. Boes and H. Zuchner, *J. Less-Common Met.*, **49**, 223 (1976).
29. B. S. Chaudhari and T. P. Radakrishnan, *Corros. Sci.*, **30**, 1219 (1990).
30. H. A. Duarte, G. Zheng, B. N. Popov, and R. E. White, *Corros. Sci.*, Submitted.
31. R. N. Iyer and H. W. Pickering, *Ann. Rev. Mater. Sci.*, **20** (1990).
32. P. Subramanian, *Comprehensive Treatise of Electrochemistry*, Vol. 4, J. O'M. Bockris, B. E. Conway, E. A. Yeager, and R. E. White, Editors, p. 411, Plenum Press, Inc., New York (1981).